ELSEVIER

Applied Surface Science 78 (1994) 123–132

applied surface science

Mechanism of the reaction of WF_6 and Si

P.A.C. Groenen, J.G.A. Hölscher, H.H. Brongersma *

Faculty of Physics, Eindhoven University of Technology, P.O. Box 513, 5600 MB Eindhoven, The Netherlands

(Received 10 May 1993; accepted for publication 4 March 1994)

Abstract

The Chemical Vapour Deposition (CVD) of W on Si, using WF_6(g) and Si(s), has been studied by in situ mass spectrometry combined with AES depth profiling for $p_{WF_6} = 24$ Pa and $500 < T < 650$ K. The process results in W layers with a thickness of 15–20 nm, independent of temperature. A model for the process has been proposed, based on the formation of an intermediate reaction layer, which is formed in case of an excessive WF_6 supply. A mathematical description of the model is in good agreement with the measured data. It shows that both the formation of the reaction layer and the conversion of this layer into W is performed by similar reactions.

1. Introduction

The deposition of W on Si by Chemical Vapour Deposition (CVD) has been subject to many studies because of its interest for the microelectronics industry. The base reactant in this process is the gas WF_6 that has to be converted into solid W and additional volatile products. This can be done by a range of reductants, including the Si substrate and the gases H_2, SiH_4 and GeH_4 [1–3]. When using appropriate conditions, the deposition of W occurs selectively on Si and on metallic areas, whereas no deposition occurs on SiO_2. This is advantageous for production of integrated circuits since an extra masking and etching step can be omitted.

Irrespective of the presence of additional reductants, the reaction between WF_6 and the Si substrate can always occur. In fact, this reaction will even serve as the basis for further selective growth. Moreover, because of its attractive low contact resistance, this process is often performed before supplying other reductants. A drawback of the WF_6/Si process is the consumption of Si which may cause encroachment of the existing structures. Fortunately, the process is self-protected against too much damage: once a W layer has been deposited, this layer shields the Si substrate for further reactions with WF_6. Because of the absence of the reductant (Si) from this point, the result is a W layer with a limited thickness.

This limited layer thickness has been the subject of many studies [1,4–9], leading to two different observations. One group of studies observes a final layer thickness of 15–20 nm, independent of the reaction temperature [1,4–6]. In the other group of studies the final layer thickness has an Arrhenius-type temperature behaviour, ranging from about 10 nm at 580 K to about 200 nm at

* Corresponding author. Tel.: +31 40 474281; Fax: +31 40 453587.

0169-4332/94/$07.00 © 1994 Elsevier Science B.V. All rights reserved
SSDI 0169-4332(94)00115-H

700 K [7–9]. This case has been investigated thoroughly by Leusink et al. [9], leading to a model that describes most of their observations fairly well. Their model is based on the assumption that the transport of volatile WF_6 to the substrate is the rate-limiting step in the process. Moreover, it is assumed that Si is capable of diffusing through pores in the growing W layer, thus covering the surface completely. While the layer gets thicker, the Si transport to the surface decreases gradually until it becomes less than the adsorption rate of WF_6. At that moment the pores get obstructed by deposited W and the process stops. The temperature dependence of the Si diffusion explains the Arrhenius-type temperature dependence of the final layer thickness.

However, the pore model cannot explain the temperature-independent layer thickness, which will be the subject of this paper. Based on in situ mass spectrometry analysis, it will be shown that this effect is caused by an excessive WF_6 supply, leading to a 15–20 nm thick "reaction layer" on the substrate during the growth. Once this layer has been converted into a solid W layer, the deposition process stops.

2. Experimental details

The analysis of the WF_6/Si process is performed in a specially designed, in situ time-resolved mass spectrometer set-up, which has been described elsewhere [5,6]. A schematic of the set-up is given in Fig. 1. The reactor, being of the hot-wall type, is completely made of quartz. By means of a switch valve, the WF_6 flow can be directed either to the reactor or to the bypass. The bypass and the reactor lead to two separate rotary pumps, thus preventing diffusion of the bypass flow to the reactor.

A 40 μm pinhole in the reactor wall allows in situ analysis of the gaseous composition downstream of the heated reactor part. Cryo shields that surround the mass spectrometer ensure that

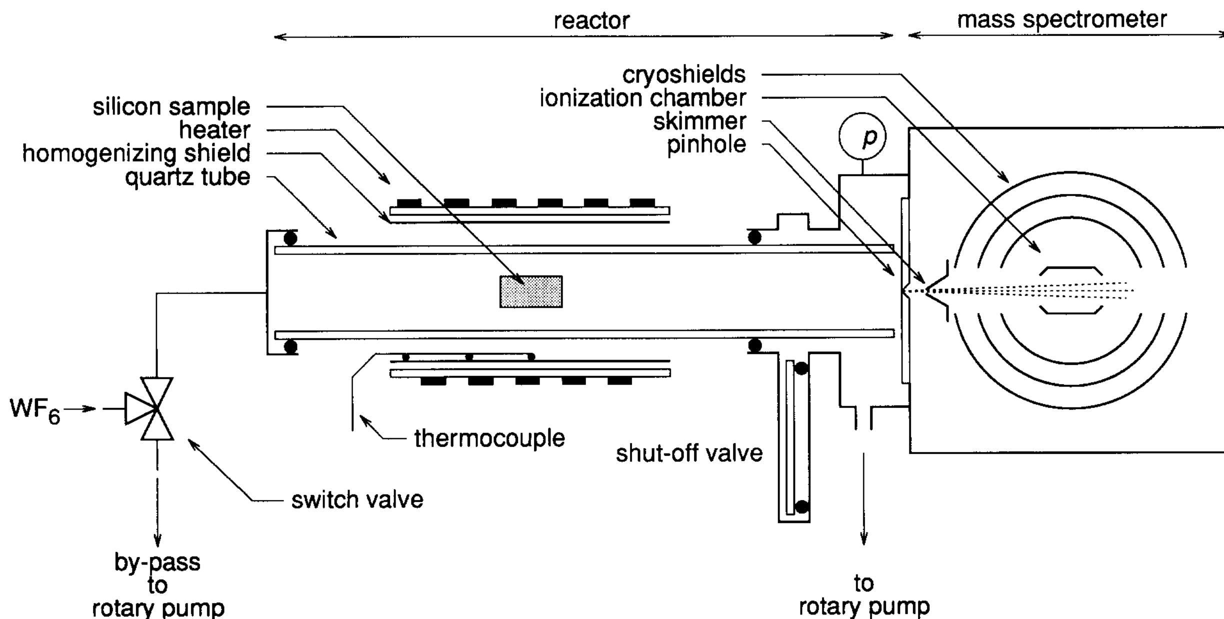

Fig. 1. Schematic of the in situ mass spectrometer set-up. The reactor is formed by a quartz tube (7 mm inner diameter) that is homogeneously heated over a length of 0.3 m. The Si sample (5×9 mm^2) is placed in the centre of the heater. By means of the switch valve, the WF_6 flow can be directed either to the reactor or to the bypass. The gas composition can be analysed via the pinhole in the quartz backwall of the reactor.

the detected molecules have not reacted with other molecules during their path from the pinhole to the ionization chamber.

Before each experiment, the quartz reactor tube is cleaned by a 5% HF solution and baked out for at least 15 h at 1000 K. This procedure is performed to remove a possible deposition of earlier experiments and to lower the water content of the reactor. The latter is checked during the experiments by monitoring the WOF_4 concentration in the reactor. This molecule, resulting from the reaction

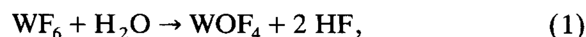

$$WF_6 + H_2O \rightarrow WOF_4 + 2\ HF, \quad (1)$$

appears to be a very sensitive indicator for the water concentration. Measurements that show a significant WOF_4 signal are rejected.

The $5 \times 9\ mm^2$ Si sample is cut out of a 4 inch Si(100) wafer (B-doped, 5–15 $\Omega \cdot cm$). Before introduction into the reactor, the sample is cleaned by an HF-etch procedure. XPS analysis of the etched Si surface shows that all SiO_2 has been removed. The Si sample is introduced into the reactor at room temperature. This is done to prevent oxidation of the Si surface that might occur while introducing the sample into the reactor at the processing temperature. After introduction of the sample an additional bake-out is performed for 30 min at 730 K and 0.1 Pa.

The experiments start by supplying a continuous pure WF_6 flow to the reactor, causing the pressure to rise to 24 Pa. In every experiment, the consumption of WF_6 is negligible with respect to its supply. The reaction temperature has been varied from 500 to 650 K. Note that our WF_6 density is much larger than in the experiments of Leusink et al. [9], who get their best results for a partial WF_6 pressure of 0.3–2 Pa in Ar. Moreover, due to thermodiffusion in their system, the partial WF_6 pressure above the sample might even be lower in their case.

As a function of time, the concentrations of WF_6, SiF_4 and WOF_4 have been measured using the mass spectrometer signals WF_5^+, SiF_3^+ and WOF_3^+, respectively. Complete mass spectra show that these are the only species of interest. Depth profiles of the deposited W layers as a function of deposition time have been taken by Auger Electron Spectroscopy (AES), combined with sputtering by Ar^+ bombardment. The total amount of W deposited has been analysed by Rutherford Backscattering Spectroscopy (RBS).

3. Results

The experimental results have been published earlier [5,6], but some of the main points are summarized below.

A typical mass spectrometer result is given in Fig. 2. As follows from the figure, the supply of

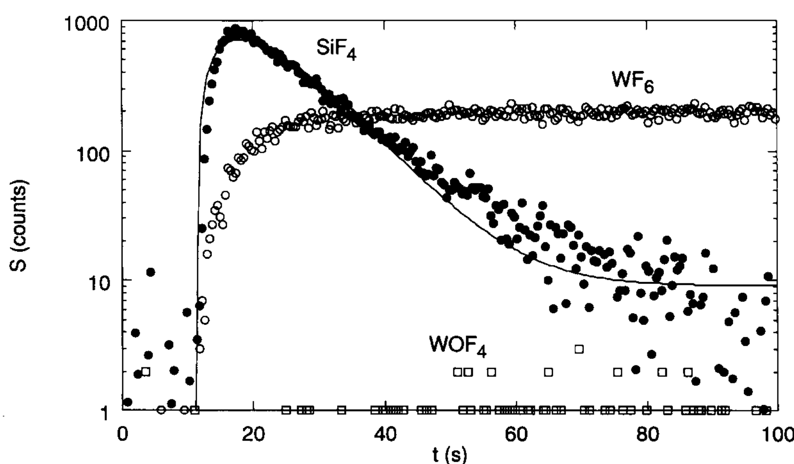

Fig. 2. Typical time-resolved mass spectrometer measurement at 575 K: (●) SiF_4, (○) WF_6, (□) WOF_4. At $t = 10$ s WF_6 is supplied to the reactor. The solid line is a result of the least-squares fit of the model $Q(t) = At\ e^{-\nu t} + B$.

WF_6 results in the formation of SiF_4. Its production increases until after a certain time a maximum has been reached. This is followed by a nearly exponential decrease of the SiF_4 production with a decay constant ν_{SiF_4}. At other reaction temperatures the behaviour of the SiF_4 production is similar to Fig. 2, the main difference being that at higher temperatures the maximum in the production is higher and reached earlier and also the exponential decay is faster, and vice versa for lower temperatures. In Fig. 3 the exponential decay constant, ν_{SiF_4}, is given as a function of the reaction temperature. As follows from the figure, ν_{SiF_4} shows an Arrhenius type temperature behaviour for deposition temperatures below 570 K, i.e.

$$\nu_{SiF_4} = \nu_0 \exp(-E/kT).$$

A linear least-squares fit of the data points below 570 K yields an activation energy of $E = 1.6 \pm 0.2$ eV and a pre-exponential value $\nu_0 = 10^{13}$ s^{-1}. The flattening of the temperature dependence for $T > 570$ K is due to experimental constraints.

An important observation is that the area under the SiF_4 curve, indicative for the total amount of SiF_4 that is produced, is independent of the temperature. This is in accordance with the observation that also the total amount of W deposited is independent of the temperature, as determined by RBS.

A typical set of AES depth profiles after various deposition times is given in Fig. 4. It is remarkable that the W concentration in the outer layers of the sample is not 100%, as would be expected on the basis of the pore model of Leusink et al. The profiles rather show that the outer 5 nm of the sample consists of a layer with a homogeneous Si and W concentration profile. During the deposition process, the Si in this layer is replaced by W. When the conversion of this layer into W is complete, the process stops and the final layer thickness has been reached. The Si concentration in the outer 5 nm appears to be directly coupled to the SiF_4 production, as shown in Fig. 5. This observation holds for the temperature regime of 500 to 650 K.

4. Model

It is obvious that the observations given above cannot be described by the pore model of Leusink et al. [9]: the layer thickness is independent of the temperature and the depth profiles contradict with the assumption of a layer-by-layer W deposition. A model that does explain our observations is presented here.

A suitable starting point for this model is the typical behaviour of the SiF_4 production, i.e., its exponential decay, and the proportionality of the SiF_4 production to the amount of Si in the outer layers. This behaviour suggests that in an early stage of the deposition process a certain volume of Si is defined, which sequentially is converted into volatile SiF_4 and metallic W. Once all defined Si has reacted, the resulting metallic W layer fully shields the Si substrate against further reactions with WF_6. The question is in what way this amount of Si, which involves some 100 atomic layers, can be determined.

A possible explanation is that after chemisorption of WF_6 on Si, the reaction of these two does not immediately result in the formation of volatile SiF_4 and W. Instead, the Si crystal will be broken

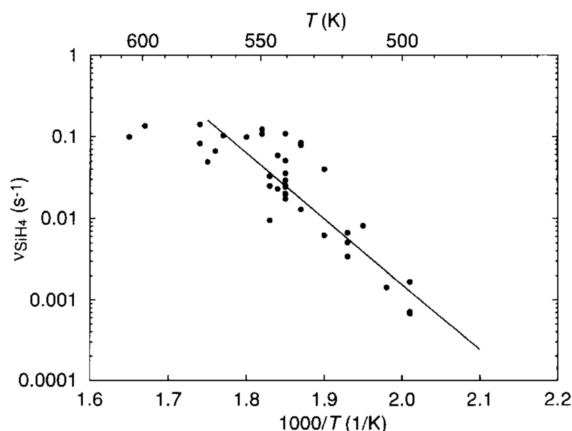

Fig. 3. Decay constant, ν_{SiF_4}, of the SiF_4 production ($Q_{SiF_4} \approx Q_0 \exp(\nu_{SiF_4} t)$ after Q_{SiF_4} has reached its maximum). The solid line is a least-squares fit to the data points at $T < 570$ K, yielding an activation energy $E = 1.6 \pm 0.2$ eV and a maximum value of 10^{13} s^{-1} for $T \to \infty$.

up and the broken bonds will be terminated by F atoms that are supplied by the WF_x species. In this way, a layer consisting of all kinds of $W_xSi_yF_z$ species will be formed. The cross-linking of the species in the layer is slowed down by the termination of the dangling bonds by F atoms.

This layer can be considered as a kind of intermediate state that will finally be converted into solid W and volatile SiF_4, and will be referred to as the "reaction layer". It is clear that the formation of the reaction layer will only occur in the case that the WF_6 supply is much faster than the production of volatile SiF_4, i.e., it will only occur in case of an excessive supply of WF_6. This is the main difference with the experiments of Leusink et al., and explains our deviating results.

It may be expected that inside the reaction layer the mobility of the various species will be relatively large. The $W_xSi_yF_z$ species will react

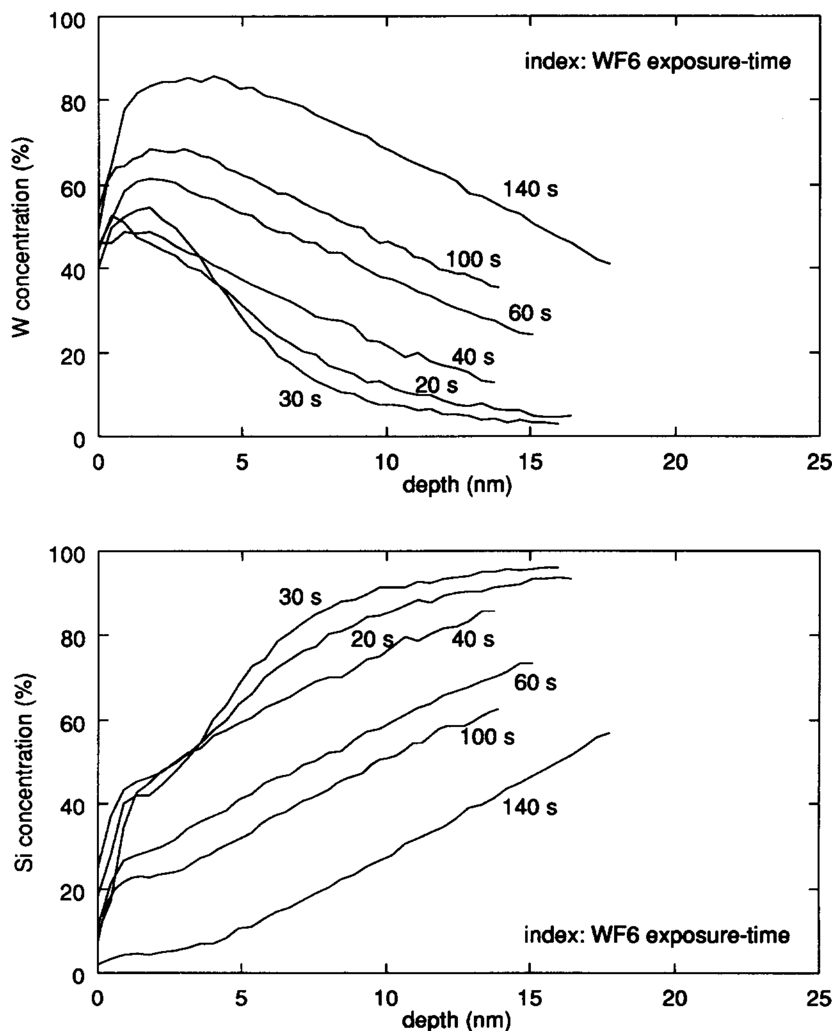

Fig. 4. AES depth profiles of W layers on Si, grown at 540 K at different WF_6 exposures. The exposure times are indicated in the figures. The depth has been estimated using a sputter yield $Y = 1.6$, being the average of the sputter yields of 4 keV Ar^+ on Si ($Y = 1.3$) and W ($Y = 1.9$) [10].

mutually and with WF_x, forming finally SiF_4 and metallic W. The formation of W–W bonds will predominate at places with a low F concentration, which are initially most likely at the interface of the reaction layer and the Si substrate. These W–W bonds will prevent both the diffusion of WF_x from the reaction layer into the substrate and the diffusion of Si from the substrate into the reaction layer. Since this process separates the reaction layer and the substrate, this is the mechanism that determines the total amount of Si that will react.

Once all Si atoms in the reaction layer have formed volatile SiF_4, the reaction stops and the F-supplying W atoms remain as the desired W layer on the Si substrate. In Fig. 6 a graphical presentation of this model is given.

The model is supported by the AES depth profiles. These show in the initial stage of the growth a fast penetration of W into the Si crystal up to a depth that is comparable with the final layer thickness. In the latter stages of the process, the penetration depth remains fixed, but the W content in the outer layers increases at the expense of the Si concentration. Moreover, the production of SiF_4 is proportional to the amount of Si in the outer layers.

The final layer thickness is determined by the ease of penetrating the Si crystal by WF_6. This will actually be an equilibrium of the formation of the reaction layer by WF_x (penetration) and the conversion of the reaction layer into volatile SiF_4 (transfer of F atoms from WF_x to SiF_y). When both processes have a comparable temperature dependence, the final layer thickness will be independent of the temperature. The observed temperature independence indicates that this is the case indeed. A possible explanation is that both formation and conversion of the reaction layer involve comparable processes, i.e., breaking up of Si–Si or Si–W bonds and transfer of F atoms.

The reaction layer concept is supported by similar observations during the etching of Si by XeF_2 [11–14]. In this case, also a kind of reaction layer is formed on top of the Si substrate, consisting of SiF_x ($x = 1–4$) species. Estimates for the layer thickness in this case range from 7 monolayers up to 15 nm.

5. Mathematical description

A complete mathematical description of the model would require that the production and reactions of all kinds of $W_xSi_yF_z$ species, together with their concentration and diffusion through the reaction layer are taken into account. Be-

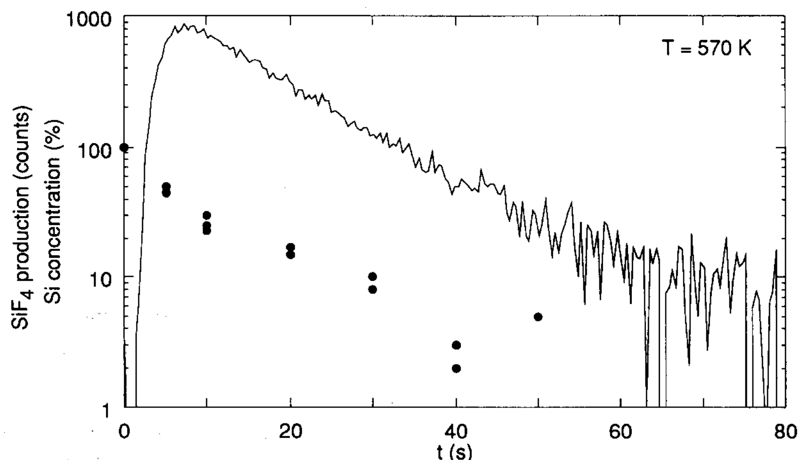

Fig. 5. SiF_4 signal (solid line) and Si concentration in the outer layers (●) as a function of the WF_6 exposure.

cause this description is very complicated, only a very simplified mathematical description of the model will be given, which will be compared to the measurements. The assumptions on this simplified description are:

- The reaction layer thickness is fixed and determined a priori.
- Species are homogeneously distributed in the reaction layer.
- Supply of WF_6 is never rate-limiting.
- There is only one type of intermediate species, indicated as W_xSiF_4.

The a priori assumption of a fixed layer thickness is based on the observation that in any case a limited layer thickness is found and that the AES depth profiles indicate a fixed penetration depth that is reached in an early stage of the process. In spite of this restriction, it can be made plausible that the process is independent of the temperature, as will be shown.

The involved reactions are the formation of W_xSiF_4 from WF_6 and crystalline Si,

$$Si + xWF_6 \rightarrow W_xSiF_4, \quad (2)$$

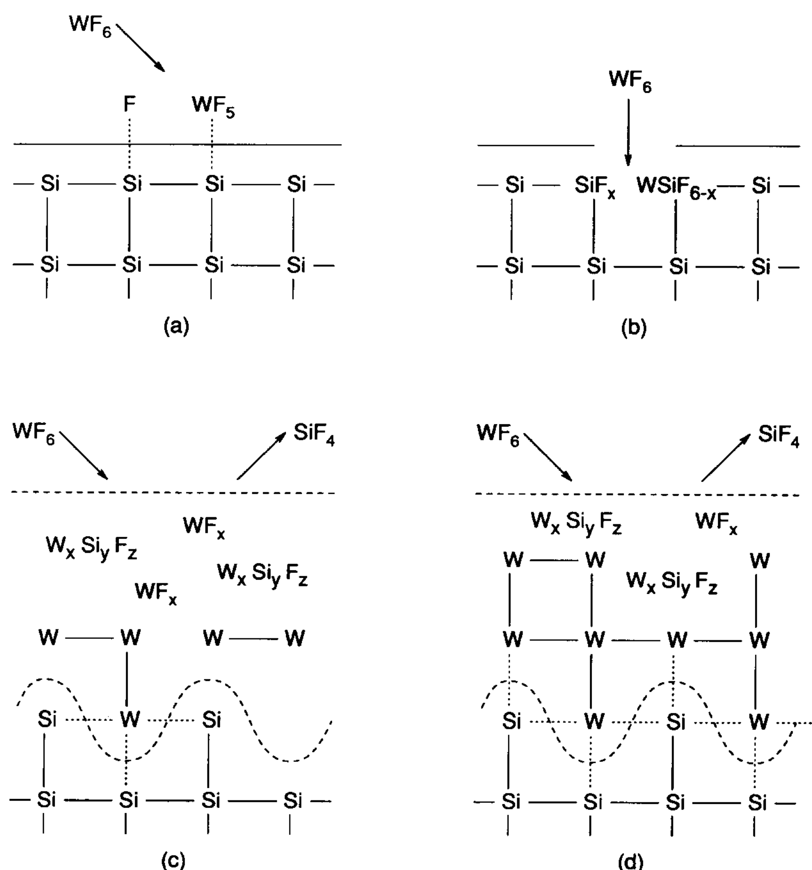

Fig. 6. Schematic of the model for the reaction of WF_6 and Si, involving an intermediate reaction layer. Four stages are given: (a) Dissociative adsorption of WF_6. (b) Break-up of Si crystal and penetration of WF_6 into the substrate. (c) Formation of a reaction layer involving all kinds of $W_xSi_yF_z$ species. At the interface of the reaction layer W–W bonds will be formed because of a depletion of F atoms. The dashed curve indicates that this interface is not necessarily sharp. (d) The clustered W atoms prevent further extension of the reaction layer. The reaction layer will be converted into metallic W and volatile SiF_4.

and the conversion of W_xSiF_4 into solid W and volatile SiF_4,

$$W_xSiF_4 \rightarrow xW + SiF_4. \quad (3)$$

Stoichiometry demands that $x = \frac{2}{3}$, indicating that the final amount of deposited W atoms is a fraction of $\frac{2}{3}$ of the amount of consumed Si. Conservation of the amount of particles in the layer, N_{tot}, is described by

$$N_{tot} = N_{Si} + N_{W_xSiF_4} + x^{-1}N_W, \quad (4)$$

where the indices Si, W_xSiF_4 and W indicate unreacted Si, intermediate W_xSiF_4 and solid W, respectively. The production and conversion of W_xSiF_4 is described by

$$dN_{W_xSiF_4}/dt = \nu_p N_{Si} - \nu_c N_{W_xSiF_4}, \quad (5)$$

where ν_p and ν_c are the rate constants of production and disproportionation of W_xSiF_4, respectively. The production of SiF_4, Q_{SiF_4}, is equal to the amount of converted W_xSiF_4. Because together with the volatile SiF_4 also x solid W atoms are produced, Q_{SiF_4} is also proportional to the growth of the number of W atoms,

$$Q_{SiF_4} = \frac{1}{x}\frac{dN_W}{dt} = \nu_c N_{W_xSiF_4}. \quad (6)$$

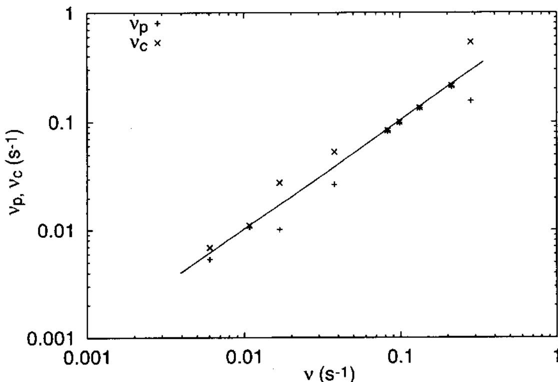

Fig. 7. Comparison of the resulting parameters ν_p and ν_c from fitting Eq. (9) (when possible) and parameter ν from fitting Eq. (8). As expected, $\nu_p \approx \nu_c \approx \nu$ (solid line).

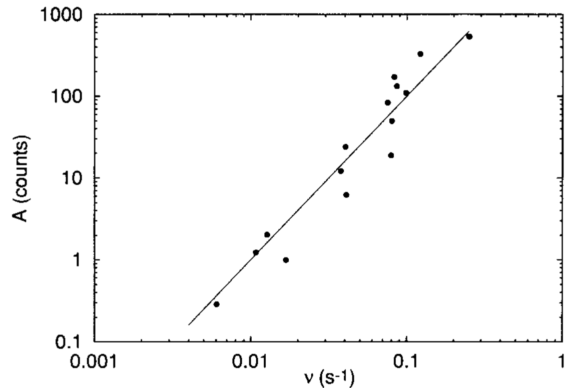

Fig. 8. Relation between the fit parameters A and ν from the least-squares approximation of the function $Q = At\ e^{-\nu t} + B$ for all measurements. As expected, $A \propto \nu^2$, which is indicated by the solid line.

Solution of these equations yields

$$Q_{SiF_4} = \begin{cases} N_{tot}\nu^2 t\ e^{-\nu t} \\ \quad \text{for } \nu = \nu_p = \nu_c, \\ N_{tot}\dfrac{\nu_c \nu_p}{\nu_c - \nu_p}(e^{-\nu_p t} - e^{-\nu_c t}) \\ \quad \text{for } \nu_p \neq \nu_c. \end{cases} \quad (7)$$

Both solutions are compared to the measured data by a non-linear least-squares approximation of the functions

$$Q = At\ e^{-\nu t} + B \quad (8)$$

$$Q = A(e^{-\nu_p t} - e^{-\nu_c t}) + B. \quad (9)$$

When fitting Eq. (9), starting with different values for ν_p and ν_c, both parameters approach each other more closely after each iteration step, indicating that $\nu_p \approx \nu_c$. At the same time the parameter A increases to extremely large values, often causing a numerical overflow. This is obvious as from Eq. (7) follows that parameter A of fit function equation (9) contains a division by $(\nu_c - \nu_p)$. Eq. (7) shows that in this case the other solution, being fit function equation (8), has to be used. Fitting Eq. (8) does not give any numerical overflow. The resulting parameter ν is approximately equal to the parameters ν_p and ν_c that followed from fitting Eq. (9), as shown by Fig. 7. An example of such an approximation is given in

Fig. 2. The model predicts that the parameter A of Eq. (8) is proportional to ν^2, which is true indeed as shown in Fig. 8.

The main conclusion of this mathematical approach is that both production and conversion of the reaction layer show a comparable temperature behaviour. It is, therefore, very likely that both processes involve similar reactions. The model further indicates that the experimentally observed exponential decay constant, ν_{SiF_4} (Fig. 3) is actually the rate constant for the production and conversion of the reaction layer. This explains the Arrhenius-type behaviour of the decay constant and yields the activation energy for the reactions. Moreover, the resulting pre-exponential value $\nu_0 \approx 10^{13}$ s^{-1} is the typical frequency for first-order solid-state reactions, which supports the model.

In the previous section it was proposed that the final layer thickness is determined by an equilibrium between the production and conversion of an intermediate species. The result that these two processes have a comparable temperature behaviour makes it more plausible that this final layer thickness is independent of the reaction temperature.

6. Summary

The CVD of W on Si by the reaction of WF_6 and Si has been studied by in situ time-resolved mass spectrometry for the case of excessive WF_6 supply ($p_{WF_6} = 24$ Pa) and for the temperature interval $500 < T < 650$ K. The deposited layers have been analyzed by RBS and AES depth profiling as a function of the deposition time. The deposition process results in W layers with a thickness of 15–20 nm, independent of the reaction temperature.

The in situ mass spectrometry shows a typical and very temperature-sensitive behaviour of the SiF_4 production as a function of time. This SiF_4 production is characterized by a temperature-dependent start-up process, followed by an exponential decay. The AES depth profiles show that the initial stage of the process is characterized by the in-depth growth of W. In the later stages of the process, the penetration depth remains fixed and the Si in the outer layers is replaced by W. Moreover, the concentration profiles in the outer layers appear to be rather homogeneous.

A model is proposed, based on the formation of an intermediate reaction layer on top of the Si substrate in the initial stage of the process. A prerequisite for the formation of this layer is an excessive WF_6 supply. In the later stages of the process, this layer is converted into volatile SiF_4 and solid W. A mathematical description of this model is in good agreement with the measured data. It yields that the reactions that produce the intermediate reaction layer and the reactions that convert this layer into volatile SiF_4 and solid W are similar.

Acknowledgements

This work forms part of the "Innovatief Onderzoeks Programma IC Technologie" (Innovative Research Program for IC Technology) and was made possible by financial support from the Dutch Ministry of Economic Affairs. The investigations were also supported by the Netherlands' Foundation of Chemical Research (SON) with financial aid from the Netherlands' Organization for the Advancement of Scientific Research (NWO).

References

[1] E.K. Broadbent and C.L. Ramiller, J. Electrochem. Soc. 131 (1984) 1427.
[2] R.S. Rosler, J. Mendonca and M.J. Ria, J. Vac. Sci. Technol. B 6 (1988) 1721.
[3] C.A. van der Jeugd, G.J. Leusink, G.C.A.M. Janssen and S. Radelaar, Appl. Phys. Lett. 57 (1990) 354.
[4] M.L. Hitchman, A.D. Jobson and L.F.Tz. Kwakman, Appl. Surf. Sci. 38 (1989) 312.
[5] P.A.C. Groenen, J.G.A. Hölscher and H.H. Brongersma, Appl. Surf. Sci. 53 (1991) 30.
[6] P.A.C. Groenen, J.G.A. Hölscher and H.H. Brongersma, J. Phys. IV (1991) 185.
[7] M.L. Yu, B.N. Eldridge and R.V. Joshi, in: Proc. Workshop on Tungsten and Other Refractory Metals for VLSI

Applications IV, Eds. R.S. Blewer and C.M. McConica (MRS, Pittsburgh, PA, 1989) p. 221.
[8] A.E.T. Kuiper, M.F.C. Willemsen and J.E.J. Schmitz, Appl. Surf. Sci. 38 (1989) 338.
[9] G.J. Leusink, C.R. Kleijn, T.G.M. Oosterlaken, G.C.A.M. Janssen and S. Radelaar, J. Appl. Phys. 72 (1992) 490.
[10] R. Behrisch, in: Sputtering by Particle Bombardment I, Vol. 47 of Topics in Applied Physics (Springer, Berlin, 1981) pp. 169, 185.
[11] J.A. Yarmoff and F.R. McFeely, J. Appl. Phys. 63 (1988) 5213.
[12] F.R. McFeely, J.F. Morar and F.J. Himpsel, Surf. Sci. 165 (1986) 277.
[13] H.F. Winters and D. Haarer, Phys. Rev. B 36 (1987) 6613.
[14] G.J.P. Joosten, M.J.M. Vugts and H.C.W. Beijerinck, private communication.